



Article

β -Cyclocitral-Mediated Metabolic Changes Optimize Growth and Defense Responses in *Solanum lycopersicum* L.

Shreyas Deshpande and Sirsha Mitra *

Department of Botany, Savitribai Phule Pune University, Pune 411007, India

* Correspondence: smitra@unipune.ac.in

Abstract: β -cyclocitral (β CC) is one of the significant oxidative products of β -carotene. It primes plants for multiple stress acclimation without compromising plant growth. Metabolic reorganization is necessary to maintain a balance between growth and defense. However, the β CC-mediated changes in a plant's metabolic network are unknown. Here, we demonstrate how β CC-induced metabolic changes enable *Solanum lycopersicum* L. (tomato) plants to promote defense and maintain growth under stress. An analysis of early (0–240 min) and late (72 h) changes in the tomato metabolome after β CC-treatment using liquid chromatography and tandem mass spectrometry identified 57 compounds. A principal coordinate analysis suggested that β CC treatment significantly changes the metabolite profile. A variable importance in projection (VIP) analysis revealed 16 and 19 discriminant metabolites from early and late samples, respectively (VIP \geq 1.0). Upregulated metabolites were mainly amino acids and phytophenols. Pathway enrichment analysis showed that β CC treatment influenced amino acid metabolism at early and later times; however, phenylpropanoid and isoquinoline biosynthesis were influenced only at the later time. A 66.6% similarity in the upregulated metabolites of β CC- and simulated-herbivory-treated plants confirmed β CC's role against herbivores. We conclude that β CC steers a temporal separation in amino acids and defense metabolite accumulation that optimizes resource allocation to growth and defense.



Citation: Deshpande, S.; Mitra, S. β -Cyclocitral-Mediated Metabolic Changes Optimize Growth and Defense Responses in *Solanum lycopersicum* L. *Metabolites* **2023**, *13*, 329. <https://doi.org/10.3390/metabo13030329>

Academic Editors: Shitou Xia and Junxing Lu

Received: 28 January 2023

Revised: 14 February 2023

Accepted: 18 February 2023

Published: 23 February 2023



Copyright: © 2023 by the authors. Licensee MDPI, Basel, Switzerland. This article is an open access article distributed under the terms and conditions of the Creative Commons Attribution (CC BY) license (<https://creativecommons.org/licenses/by/4.0/>).

Keywords: apocarotenoids; herbivory; liquid chromatography-mass spectrometry; metabolomics; stress signaling

1. Introduction

Environmental stresses are deleterious for the survival of plants. *Solanum lycopersicum* L. (tomato), one of the major food crops in the family Solanaceae, is also challenged by multiple environmental stresses, namely fungal pathogens, herbivores, cold, drought, etc. [1,2]. To counteract environmental challenges, plants optimize their defense strategies via stress sensing, signaling, and reorganizing their metabolic profile under the environmental stimuli. The chloroplast plays a central role in plant defense signaling as it harbors biosynthetic pathways of significant defense metabolites; chloroplast-associated carotenoids are crucial for protecting the photosynthetic apparatus from photo-oxidative damage [3] because the presence of a C40 polyene backbone makes carotenoids susceptible to oxidative cleavage. Cleavage of carotenoids occurs enzymatically by carotenoid cleavage dioxygenase or non-enzymatically by reactive oxygen species (ROS). The oxidative carbonyl products of carotenoids are known as apocarotenoids [4,5]. Apocarotenoids are well known as the precursors of abscisic acid, a phytohormone involved in abiotic stress responses [6]. In recent years, the identification of novel apocarotenoids has established their role in stress signaling [5,7]. Previous studies showed that singlet oxygen (${}^1\text{O}_2$)-mediated cleavage of β -carotene produces many apocarotenoids, where β -cyclocitral (β CC) is the major apocarotenoid [8].

Interestingly, drought, photooxidative stress, and herbivory increase the level of β CC [9–12]. Studies have shown that exogenous application of β CC can induce ${}^1\text{O}_2$ -responsive genes, marker genes for photo-oxidative stress [8]. Recently, we found that β CC

treatment triggers the accumulation of transcripts related to both abiotic and biotic stresses. Our study also revealed that exogenous application of β CC primes plants against drought and develops resistance against herbivory [11,13]. These results suggest that β CC causes functional changes in addition to transcriptomic changes. On the other hand, β CC treatment enhances the growth of primary roots and the branching of lateral roots [11]. As defenses are costly, a trade-off between growth and defense is often evident in stress-exposed plants. However, β CC treatment enhances both plant growth and defense. Metabolites can influence plant growth, the branching pattern of roots and shoots, the size, shape, and position of leaves, etc. [14–16]. Therefore, metabolic reorganization is a prerequisite to maintaining a balance between growth and defense. However, β CC-mediated changes in the plant metabolome are yet to be revealed.

In the ‘omics’ field, metabolomics identifies large-scale changes in the plant metabolome. It is highly challenging, as plant metabolites possess different physical and chemical properties and vary significantly in their concentrations [17]. Metabolomics can be investigated using two main approaches: targeted and untargeted [18,19]. Initially, chromatographic techniques, such as liquid chromatography (LC) and gas chromatography (GC), separate the metabolites, and mass spectroscopy (MS) investigates the quantitative changes in the plant metabolome [20]. The use of nuclear magnetic resonance (NMR) spectroscopy is also evident in metabolomics analysis [21]; however, as the sensitivity of MS is high, it is preferred over NMR spectroscopy for analyzing plant metabolites [22]. The tomato has been considered a model fruit. Its metabolomic profiles have been studied to discriminate different varieties, determine geographical origin, examine fruit development and ripening, and investigate seasonal changes [23]. A comparative metabolomics study of *Ralstonia solanacearum*-infected tomato leaves, stems, and roots revealed the metabolic changes after being infected with *R. solanacearum* [24]. This study identified the metabolites providing plant defense against *R. solanacearum* [24]. However, a comparative metabolomics study of tomato plants after apocarotenoid treatment has yet to be executed.

In light of the reported results and previous findings, we hypothesized that β CC treatment reorganizes plants’ metabolic networks to enhance plant growth and defense. Therefore, in the current study, we aimed to reveal how exogenous application of β CC changes the metabolic signature of the tomato plants that enables them to maintain growth under stress using an LC–MS-based approach.

2. Materials and Methods

2.1. Plant Material, Growth Conditions, and Treatments

Seeds of tomato (var. Pusa Ruby) were germinated on cocopeat. 15-day-old seedlings were transferred in pots (9 cm × 9 cm) that contained soil, cocopeat, and vermiculite (5:4:1) and raised for five weeks. These plants were treated with 1 mL of pure β CC (treatment), or water (control) kept in a watch glass in a transparent, closed glass container [11,25]. Tissues were harvested in liquid nitrogen 0, 30, 60, 90, 180, 240 min, and 72 h after treatment. Insect herbivory was simulated in tomato plants by wounding the tomato leaves with a fabric pattern wheel parallel to the mid-vein and applying 20 μ L of oral secretion of *Spodoptera litura* larvae diluted with sterile water (1:1) to the wound [26]. Tissues were harvested in liquid nitrogen 72 h after treatment. All harvested tissues were stored at –80°C until further use.

2.2. Extraction of Metabolites and Data Acquisition in LC-QTOF-MS/MS

Leaf samples of tomato plants were pulverized in liquid nitrogen. An amount of 200 mg of tissue was extracted with 1 mL methanol spiked with the internal standard formononetin (10 μ g ml^{-1}) by vortexing continuously for 15 min. Further, the extracts were centrifuged at 15,000 × g at 4 °C for 20 min. The collected supernatant was filtered and subjected to LC-QTOF-MS/MS (Agilent Technologies, Stuttgart, Germany) for analysis.

The extracts were separated on an XDB-C18 column (150 mm × 4.6 mm × 5 μ m; Agilent Zorbax-Eclipse) using 0.1% (v/v) formic acid (solvent A) and acetonitrile with

0.1% formic acid (solvent B) as mobile phases. Compounds were eluted with a solvent gradient profile consisting of 95% A for 1 min followed by a gradient that reached 95% B by 15 min, returned 95% A by 17.5 min, and continued until 20 min. The injection volume was adjusted to 10 μ L. The eluted compounds were detected using the centroid mode for both negative and positive ionization modes. The pump limit was 1 min; the draw speed and eject speed were set to 200 μ L min $^{-1}$ and 400 μ L min $^{-1}$, respectively. The maximum pressure limit in the column was 800 bar, and the retention time exclusion tolerance was set to (\pm) 0.2 min. The ion source (dual ESI) was adjusted with a limit of 2 precursors min $^{-1}$.

2.3. LC-QTOF-MS/MS Data Analysis

Initially, a personal compound database library (PCDL) was prepared by accessing different databases and libraries for the metabolites from Solanaceae plants. The PCDL library and the Mass Hunter Qualitative Analysis BO.07.00 tool (Agilent Technologies) were used to analyze the spectra of the metabolites. The MS/MS data were procured from four replicate samples to assess the biological variations in the control, β CC-, and simulated-herbivory-treated samples. Compounds with an abundance greater than 10,000 counts and a score of more than 75 were considered for further analysis. These compounds were identified with a mass threshold of 7 ppm and a peak distance threshold of 10 ppm in MS/MS mode using the ‘find by formula’ function in the Mass Hunter software. The molecular ion and daughter ions in MS and MS/MS modes were compared with the reference or predicted spectra available at the Human Metabolome Database (HMDB), MassBank, and Pubchem.

2.4. Statistical Analysis

Principal coordinate analysis (PCoA) of metabolomics data was performed in PAST 3 [27]. A heatmap was prepared with the web tool ClustVis (<https://biit.cs.ut.ee/clustvis/>; accessed on 1 December 2022). Metaboanalyst 5.0 (<https://www.metaboanalyst.ca/>; accessed on 1 December 2022) was used for orthogonal partial least square discriminant analysis (OPLS-DA), variable importance in projection (VIP), fold-change analysis, and pathway analysis. Venn diagrams were created using Venny 2.1 (<https://bioinfogp.cnb.csic.es/tools/venny/>; accessed on 1 December 2022) [28]. Normalized peak areas were analyzed by one-way ANOVA followed by Fisher’s least significant difference (LSD) post hoc test. The significance was determined at $p \leq 0.05$.

3. Results

3.1. Application of β CC Altered the Metabolite Profile of Tomato Plants

Previous reports showed that exogenous β CC could improve plants’ tolerance to different stresses but did not reduce plant growth [9,11]. Therefore, to investigate how β CC improves plants’ tolerance without compromising plant growth, we analyzed the metabolome of tomato plants after β CC treatment and compared it with control plants. Samples were collected at 0, 30, 60, 90, 180, and 240 min after β CC treatment to assess β CC-mediated early changes in the metabolome (Figure S1). Similarly, to track the β CC-induced late metabolic changes, samples were collected at 72 h after β CC treatment (Figure S1). A total of 57 compounds were identified from positive and negative modes across all the time points. Compounds were identified based on the daughter ion spectra at three energy levels 10 eV, 20 eV, and 40 eV (Table S1). Among the identified compounds, 45 and 31 were accumulated at early (0–240 min) and late (72 h) time points, respectively. A heatmap created with the identified compounds showed that the metabolic profiles of β CC-treated samples differed from that of the control (Figure 1a). Principal coordinate analysis (PCoA) showed a total variability of 70.35%, where the maximum variation was captured in coordinates 1 (44.67%) and 2 (25.68%). Interestingly, β CC-treated samples from 0–240 min were grouped separately from the control samples from the same time points (0–240 min). However, the control and β CC-treated samples from 72 h were grouped in

the same coordinate in the PCoA plot (Figure 1b). This suggests that β CC-mediated early changes in the metabolite profile were more prominent than later changes.

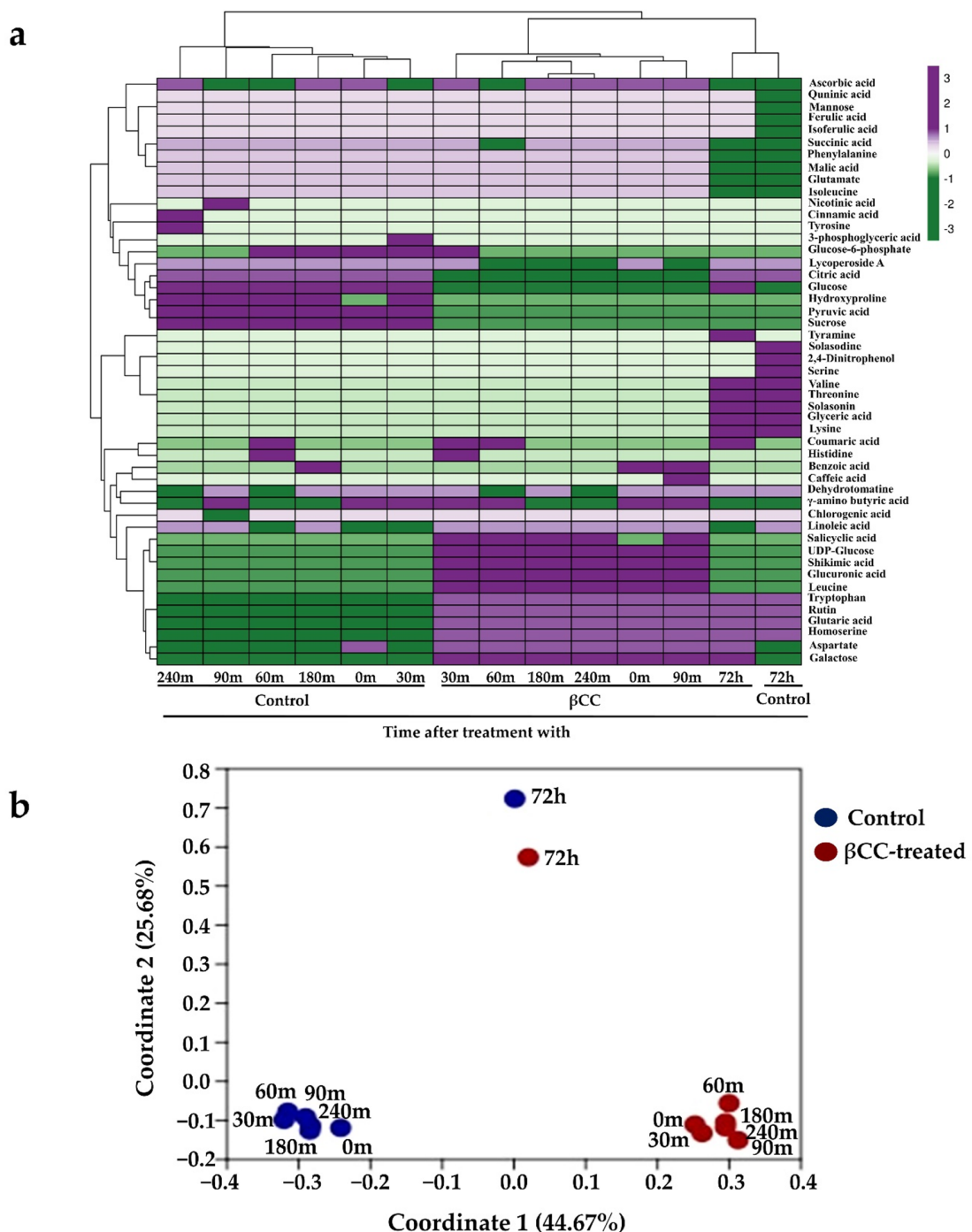


Figure 1. Variation in the metabolites after β CC treatment across different time points. (a) The metabolites showed variation in their accumulation pattern across different time points after being treated with β CC. The color scheme at the top-right corner codes for the z-scores (-3 to $+3$) calculated over binary coordinates of the samples. The average linkage clustering computed between the samples is based on the Manhattan distance and depicted at the top of the heatmap. (b) The principal coordinate analysis (PCoA) was performed with the identified metabolites using the Jaccard coefficient and transformation exponent value 2. It showed that the maximum percentage of the variation was captured in coordinates 1 and 2. The values in parentheses show the percentages of the variation.

3.2. Regulation of Metabolites in Early Time Points after β CC Treatment

The PCoA plot indicated a pronounced effect of β CC on metabolite accumulation within 0–240 min after the treatment. To find out the discriminant metabolites that were responsible for separating the control and β CC-treated samples, the peak area of 45 identified compounds from 0–240 min time scale were normalized with the internal standard and analyzed for an orthogonal partial least square discriminant analysis (OPLS-DA) and variable importance in projection (VIP) analysis. OPLS-DA showed that the control and β CC-treated samples were well separated in the score plot (Figure 2a). The data confirmed that the metabolic blend of the control and β CC-treated samples were different. VIP analysis determined the relative contribution of the metabolites to the variation between the control and β CC-treated samples. The analysis identified a total of 16 discriminant compounds (VIP score ≥ 1.0) (Figure 2b).

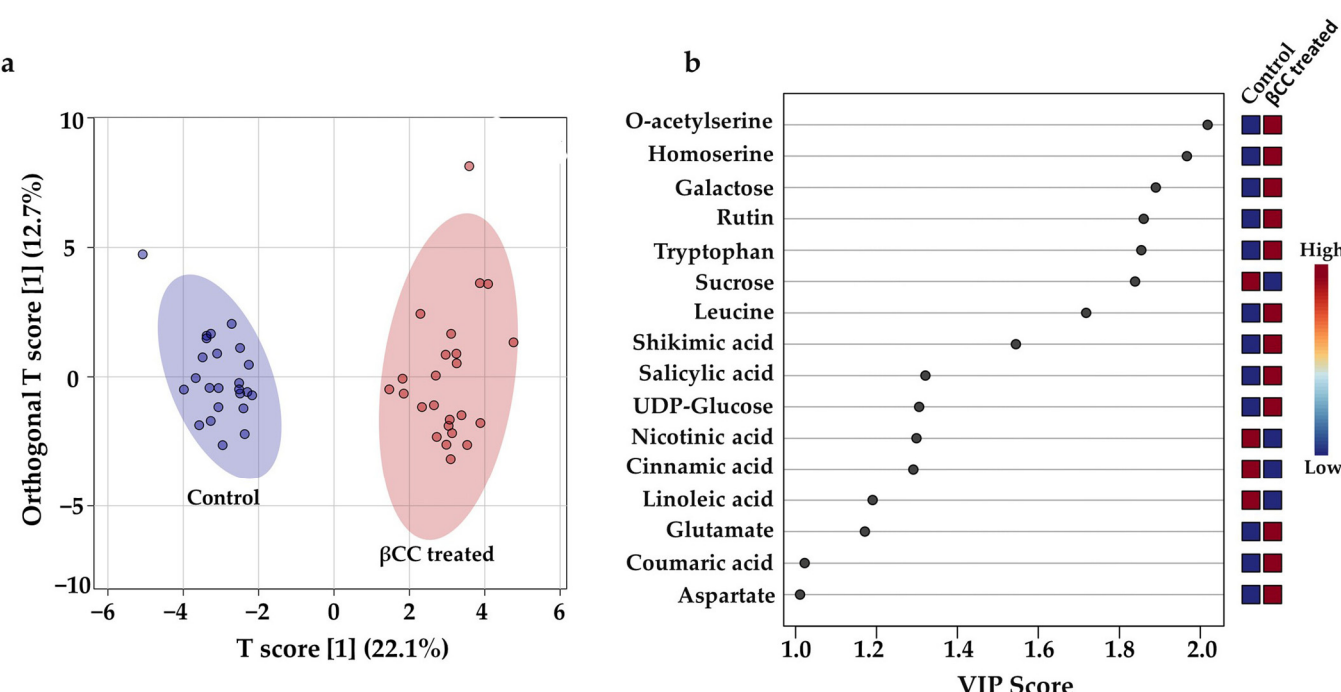


Figure 2. β CC-induced early metabolic changes and discriminant metabolites. To examine the differences in the metabolic profile in tomato plants early after β CC treatment, orthogonal partial least square discriminant analysis (OPLS-DA) and variable importance in projection (VIP) analysis were performed with the normalized peak area of the metabolites identified from 0–240 min after β CC treatment and in control plants. (a) An OPLS-DA plot showed the control group clustered to the left region and the β CC-treated group clustered to the right area in the OPLS-DA score plot. The shaded ellipses represent the confidence interval of 95% from OPLS-DA models. (b) A variable importance in projection (VIP) plot showed that the metabolites responsible for the significant separation observed between the two sample groups were indicated by a VIP score ≥ 1.0 . An increase in VIP score indicates a high contribution of the metabolites to the group separation. The red and blue boxes on the right indicate whether the metabolite concentration was high (red) or low (blue) in the β CC-treated plants compared to control plants.

Further, the fold-change analysis revealed that, out of 16 discriminant compounds, 11 were upregulated ($\log_2\text{FC} \geq 2$), and four were downregulated ($\log_2\text{FC} \leq -2.0$) (Figure S2). Though the $\log_2\text{FC}$ value of one of the discriminant metabolites (aspartate) was 1.8, its VIP score was 1.01; therefore, it had the most negligible influence in separating the control and β CC-treated sample groups. The normalized peak area of the discriminant metabolites from all the time points was further analyzed by one-way ANOVA and Fisher's LSD post hoc test. Significantly different metabolites were determined at $p \leq 0.05$ (Table S2)

and visualized by mapping their regulation in the network of metabolic pathways for each time point (Figure 3a). The analysis showed that the upregulated metabolites were mainly amino acids and their derivatives (i.e., tryptophan, leucine, aspartate, glutamate, homoserine, and o-acetylserine), followed by phytophenols (i.e., shikimate, rutin, and coumaric acid), carbohydrates and their derivatives (i.e., UDP-glucose and galactose), and carboxylic acid (i.e., salicylic acid). Cinnamic acid, linoleic acid, nicotinic acid, and sucrose were significantly downregulated metabolites. Most of the compounds were upregulated, so a pathway enrichment analysis was performed with the upregulated compounds. It revealed that the pathways related to (1) aminoacyl-tRNA biosynthesis ($p = 0.0001$), (2) glycine, serine, and threonine metabolism ($p = 0.001$), (3) lysine biosynthesis ($p = 0.0010$), (4) cysteine and methionine metabolism ($p = 0.0028$), (5) arginine biosynthesis ($p = 0.0059$) (6) phenylalanine, tyrosine, and tryptophan biosynthesis ($p = 0.0088$), (7) alanine, aspartate, and glutamate metabolism ($p = 0.0088$) (8) galactose metabolism ($p = 0.0131$), and (9) indole alkaloid biosynthesis ($p = 0.0267$) were significantly influenced (hypergeometric test; $p \leq 0.05$) by β CC application (Figure 3b). The above data suggest that β CC treatment mainly boosted plants' amino acid metabolism within a few hours of treatment.

3.3. Regulation of Metabolites at a Late Time Point after β CC Treatment

Generally, in plants, accumulation of defense metabolites takes place 3–4 days after exposure to stress [29]. Surprisingly, the PCoA plot indicated that the metabolic blend of β CC-treated samples from 72 h was less different than that of the control samples. This result suggests that quantitative changes were more critical than qualitative changes in later times. The Venn diagram constructed with the metabolites detected 72 h after β CC treatment showed that, among 31 identified compounds, 19 were commonly present (63%) in control and β CC-treated plants, and only eight compounds (25%) were detected explicitly after β CC treatment (Figure 4a). However, the OPLS-DA (Figure 4b) and fold-change analysis (Figure S3) showed that, though the metabolite profile of control and β CC-treated plants were qualitatively similar, they were quantitatively different. Further, we identified the discriminant metabolites from β CC-treated samples after 72 h of treatment by VIP analysis. This revealed 19 discriminant compounds, of which 15 compounds (78%) were significantly upregulated ($\log_{2}FC \geq 2.0$), and four compounds (21%) were significantly downregulated ($\log_{2}FC \leq -2.0$). The upregulated compounds included mainly phytophenols (i.e., isoferulic acid, ferulic acid, coumaric acid, and quinic acid), followed by amino acids (i.e., homoserine, threonine, valine, tyramine, and aspartate), carbohydrates and their derivatives (i.e., galactose, glucose, and mannose), organic acids (i.e., citric acid and fumaric acid), and steroid alkaloids (i.e., α -tomatine) (Figure 4c). Significantly downregulated metabolites were serine, solasodine, solasonin, and linoleic acid (Figure 4c). The pathway enrichment analysis of the upregulated discriminant compounds revealed their involvement in (1) glycine, serine, and threonine metabolism ($p = 0.0014$), (2) lysine biosynthesis ($p = 0.0017$), (3) aminoacyl-tRNA biosynthesis ($p = 0.0038$), (4) tyrosine metabolism ($p = 0.0056$), (5) arginine biosynthesis ($p = 0.0071$), (6) citrate cycle ($p = 0.0088$), (7) valine, leucine and isoleucine biosynthesis ($p = 0.0106$), (8) alanine, aspartate and glutamate metabolism ($p = 0.0106$), (9) cysteine and methionine metabolism ($p = 0.0433$), (10) phenylpropanoid biosynthesis ($p = 0.0433$), and (11) isoquinoline alkaloid biosynthesis ($p = 0.0437$) (hypergeometric test; $p \leq 0.05$) (Figure 4d). The data suggest that β CC treatment enhanced the pathways related to plant defense at later time points, keeping the amino acid biosynthesis and metabolism boosted.

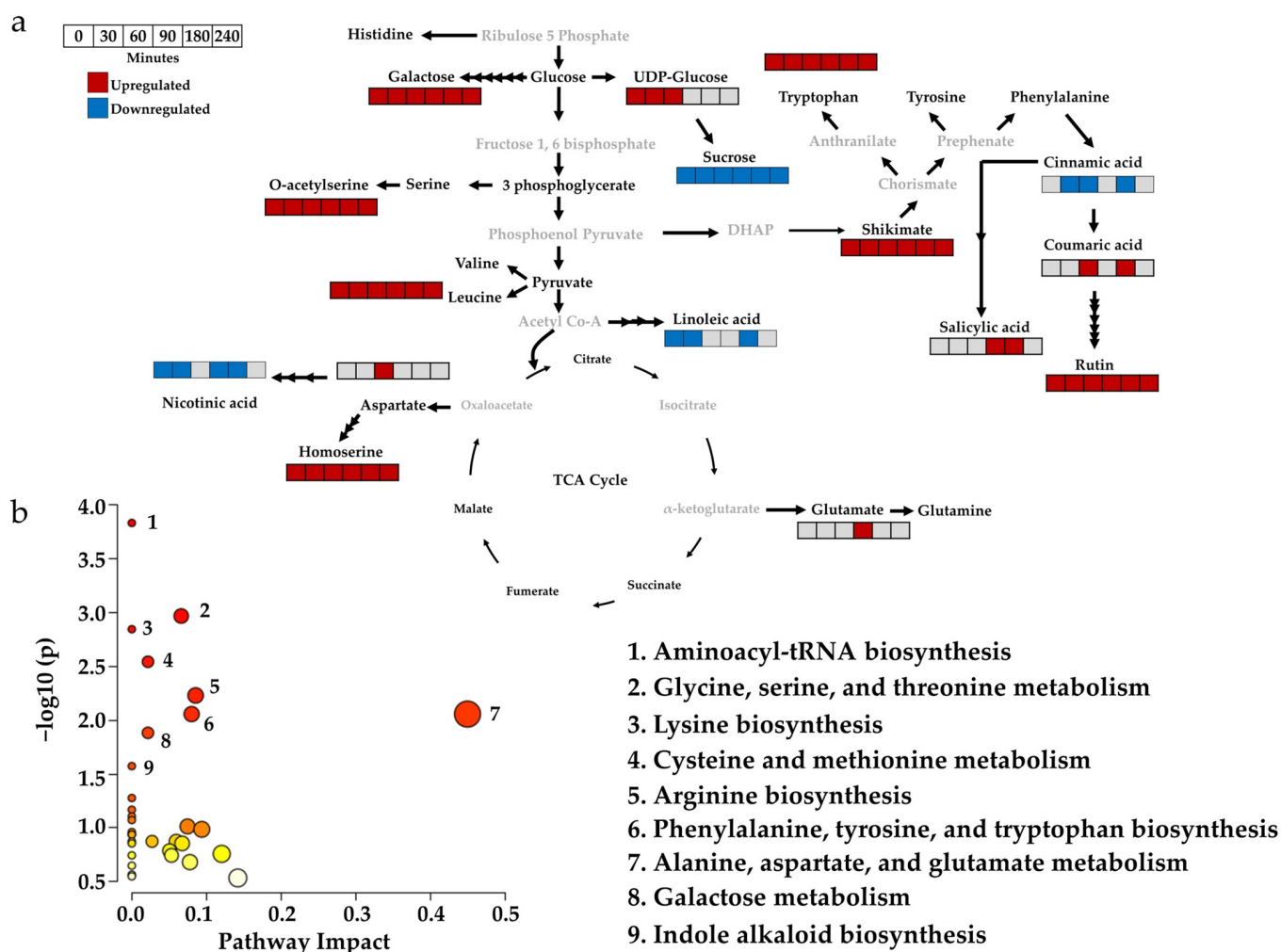


Figure 3. Mapping the relative expression of discriminant metabolites early after β CC treatment and their influence on metabolic pathways. The normalized peak area of the discriminant metabolites from control and β CC-treated samples of different time points (0, 30, 60, 90, 180, and 240 min) were subjected to one-way ANOVA; the significance was determined by Fisher's LSD at $p = 0.05$. (a) Significantly up- and down-regulated metabolites from different time points are mapped on the pathways modified from the KEGG database. (b) Pathway analysis using the upregulated discriminant metabolites shows altered pathways after β CC treatment (left panel). The x-axis depicts pathway impact values obtained from the pathway topology analysis, and the y-axis depicts the $-\log$ of the p values obtained from the pathway enrichment analysis ($p \leq 0.05$). Circular nodes represent the metabolic pathways. The size of the circular nodes positively corresponds with the impact of the proposed pathway based on the pathway topology. The node color, from yellow to orange, shows different levels of significance based on pathway enrichment analysis (yellow–low; orange–high). The most significantly altered pathways are characterized by both a high $-\log(p)$ value and a high impact value. Nine pathways were significantly altered after β CC treatment (right panel). Metabolites in black font were identified in the study, but greys were not. Grey boxes indicate no significant changes in the metabolite accumulation at $p \leq 0.05$.

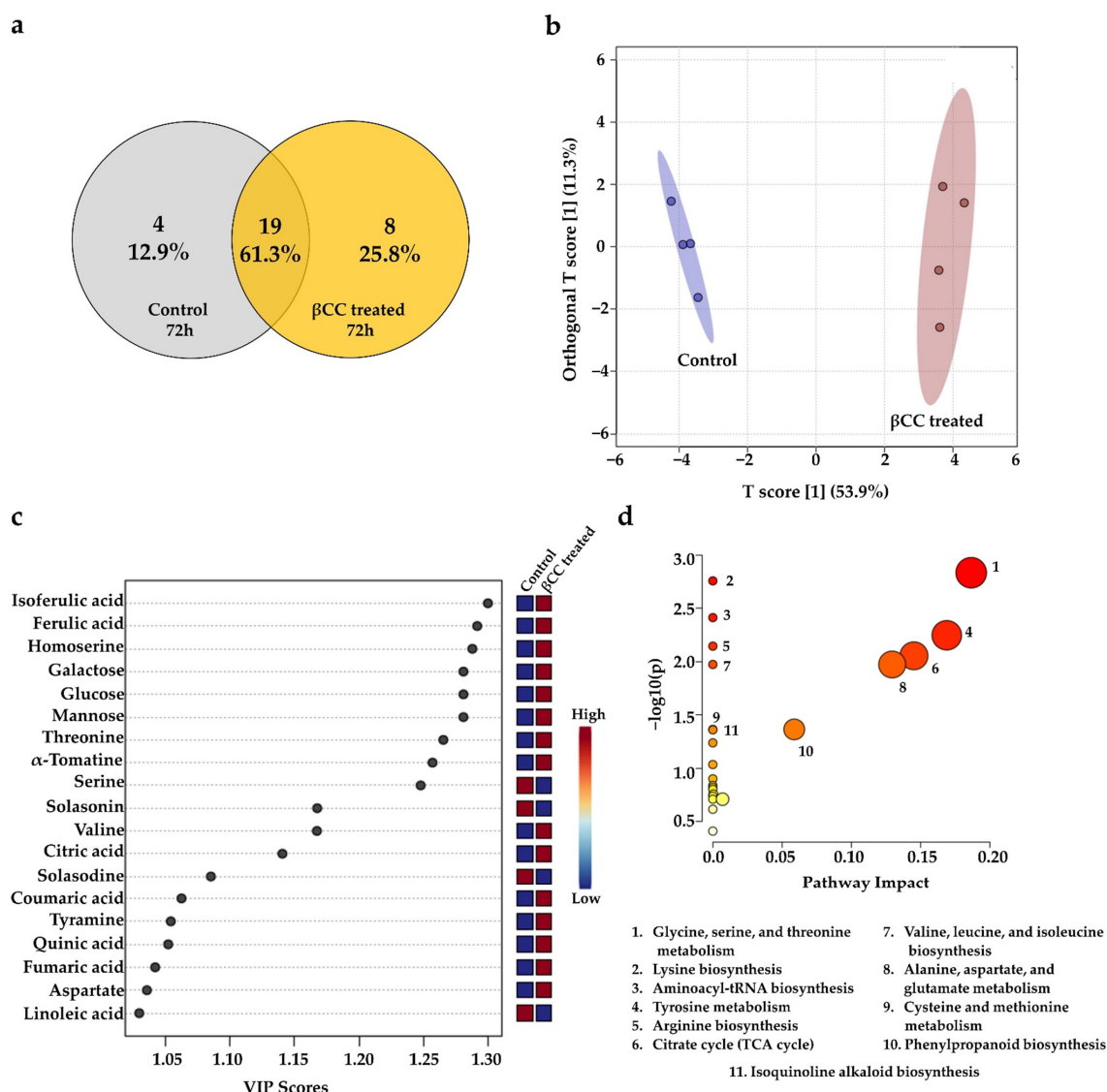


Figure 4. βCC-induced late metabolic changes, discriminant metabolites, and their influence on metabolic pathways. (a) A Venn diagram created with the identified metabolites from control and βCC-treated samples showed many metabolites regulated commonly and specifically in them. (b) OPLS-DA plot showed distinct clusters of the control group to the left region and the βCC-treated group to the right region of the plot. The shaded ellipses represent the confidence interval of 95% from OPLS-DA models. (c) A variable importance in projection (VIP) plot showed that the metabolites responsible for the significant separation observed between these two sample groups were indicated by a VIP score ≥ 1.0 . An increase in VIP score indicates a high contribution of the metabolites to the group separation. The red and blue boxes on the right indicate whether the metabolite concentration was high (red) or low (blue) in the βCC-treated plants compared to control plants. (d) Pathway analysis using the upregulated discriminant metabolites shows altered pathways after βCC treatment (upper panel). The x-axis depicts pathway impact values obtained from the pathway topology analysis, and the y-axis depicts the $-\log_{10}(p)$ values obtained from the pathway enrichment analysis ($p \leq 0.05$). Circular nodes represent the metabolic pathways. The size of the circular nodes positively corresponds with the impact of the proposed pathway based on the pathway topology. The node color, from yellow to orange, shows different levels of significance based on pathway enrichment analysis (yellow—low; orange—high). The most significantly altered pathways were characterized by both a high $-\log_{10}(p)$ value and a high impact value. A total of 11 pathways were significantly altered after βCC treatment (lower panel).

3.4. β CC Treatment Induces a Similar Metabolic Response as Simulated Herbivory

Previously, we found that β CC treatment was also able to enhance resistance against a generalist herbivore, *Spodoptera littoralis*, in *Arabidopsis thaliana* [13]. To investigate if the discriminant metabolites are also influenced after insect herbivory, we compared the levels of β CC-induced metabolites with simulated-herbivory-treated and control plants after 72 h of treatment. Interestingly, out of the 15 discriminant compounds from β CC-treated plants, ten compounds (66.6%) were significantly upregulated after simulated herbivory compared to the control (Figure 5). The upregulated compounds included ferulic acid, isoferulic acid, coumaric acid, α -tomatine, tyramine, aspartate, citric acid, galactose, glucose, and mannose (Figure 5). In addition, β CC-treated samples accumulated significantly more amounts of quinic acid, threonine, valine, homoserine, and fumaric acid (One-way ANOVA; Fisher's LSD; $p \leq 0.05$) (Figure 5). The data suggest that β CC treatment can induce a similar blend of compounds that are upregulated after insect herbivory with a few more amino acids and phytophenol.

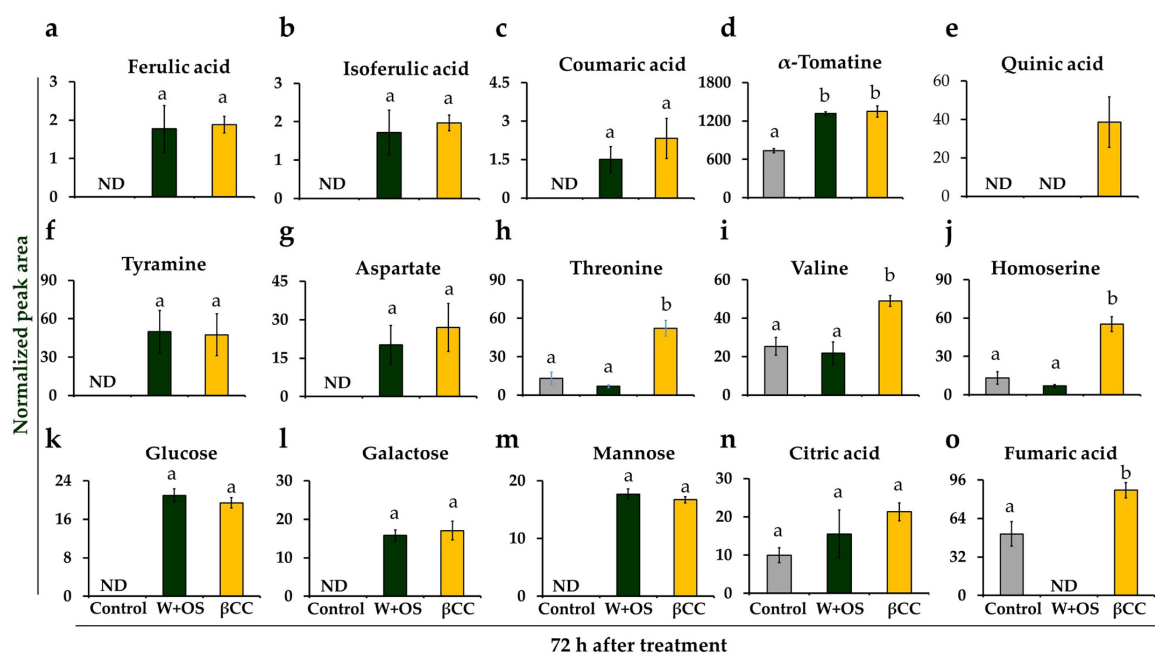


Figure 5. Comparative levels of metabolites after β CC treatment and simulated herbivory. The normalized peak area of the upregulated discriminant metabolites identified after 72 h of β CC treatment was compared with that of control and simulated-herbivory-treated (W+OS) plants. The accumulation of phytophenols, (a) ferulic acid ($F_{2,9} = 7.975$; $p_{\beta\text{CC}} = 0.006$, $p_{W+\text{OS}} = 0.008$), (b) isoferulic acid ($F_{2,9} = 9.012$; $p_{\beta\text{CC}} = 0.0036$, $p_{W+\text{OS}} = 0.0078$), (c) coumaric acid ($F_{2,9} = 5.554$; $p_{\beta\text{CC}} = 0.014$, $p_{W+\text{OS}} = 0.081$), and (d) α -tomatine ($F_{2,9} = 37.185$; $p_{\beta\text{CC}}$ and $p_{W+\text{OS}} < 0.001$) were significantly more in β CC- and simulated herbivory-treated plants, but (e) quinic acid ($F_{2,9} = 8.672$; $p_{\beta\text{CC}} = 0.0057$, $p_{W+\text{OS}} = \text{NA}$) was upregulated only after β CC treatment. Similarly, the levels of amino acids, (f) tyramine was also upregulated in β CC- and simulated-herbivory-treated plants ($F_{2,9} = 4.368$; $p_{\beta\text{CC}} = 0.034$, $p_{W+\text{OS}} = 0.027$); however, levels of (g) aspartate ($F_{2,9} = 4.082$; $p_{\beta\text{CC}} = 0.022$, $p_{W+\text{OS}} = 0.069$), (h) threonine ($F_{2,9} = 28.458$; $p_{\beta\text{CC}} = 0.0002$, $p_{W+\text{OS}} = 0.364$), (i) valine ($F_{2,9} = 10.038$; $p_{\beta\text{CC}} = 0.005$, $p_{W+\text{OS}} = 0.599$), and (j) homoserine ($F_{2,9} = 35.912$; $p_{\beta\text{CC}} < 0.001$, $p_{W+\text{OS}} = 0.341$) were upregulated only after β CC treatment. Accumulation of carbohydrates and their derivatives, (k) glucose ($F_{2,9} = 137.907$; $p_{\beta\text{CC}}$ and $p_{W+\text{OS}} < 0.001$), (l) galactose ($F_{2,9} = 33.337$; $p_{\beta\text{CC}}$ and $p_{W+\text{OS}} < 0.001$), and (m) mannose ($F_{2,9} = 260.128$; $p_{\beta\text{CC}} = 0.014$, $p_{\beta\text{CC}}$ and $p_{W+\text{OS}} < 0.001$) were also upregulated after both β CC treatment and simulated herbivory; however, accumulation of organic acids (n) citric acid ($F_{2,9} = 1.980$; $p_{\beta\text{CC}} = 0.077$, $p_{W+\text{OS}} = 0.356$), and (o) fumaric acid ($F_{2,9} = 40.004$; $p_{\beta\text{CC}} = 0.005$, $p_{W+\text{OS}} = 0.0006$) was only increased after β CC treatment. The mean normalized peak area ($\pm\text{SE}$) was analyzed from four replicate plants by one-way ANOVA and Fisher's LSD post hoc test. Different letters indicate significant differences at $p \leq 0.05$.

4. Discussion

Plant growth and productivity are severely affected by environmental stress. However, plants adapt to this unfavorable condition by optimizing their defense strategies. Therefore, the machinery of stress perception, signal transduction, and, ultimately, production of defense responses have been extensively studied. The plant hormones jasmonic acid [30], abscisic acid [31], ethylene [32], and salicylic acid [33], are known as stress signaling molecules; however, the growth hormones auxin, gibberellins, and strigolactones also participate as signaling molecules in plant–environment interactions [34]. In recent years researchers have uncovered apocarotenoids as potential signaling molecules. Studies have shown that β CC, the oxidative product of β -carotene, is a significant apocarotenoid that can induce $^{1}\text{O}_2$ -responsive genes, essential for photooxidative stress in *Arabidopsis thaliana* [8]. We found that the exogenous application of β CC reprograms the transcriptome of tomato plants [25] by triggering multiple stress-responsive genes, essential to counteract both abiotic and biotic stresses. We also found that β CC can prime tomato plants against drought and induce resistance against insect herbivores in *A. thaliana* plants [11,13]. However, β CC treatment does not negatively affect plant growth but enhances root growth and lateral branching [10,11]. Generally, plants compromise their photosynthetic ability under stress, and, at the same time, they invest in defense; this reduces the carbon flux towards growth and causes a growth–defense trade-off [35]. Previous studies on tomato metabolomics have revealed that the leaf, stem, and root metabolome present different signatures upon infestation. In addition, metabolomic markers can be used to monitor or predict the performance of plants and their response to environmental stresses [36]. These facts stimulated the hypothesis that β CC specifically upregulates those metabolites that play a dual role in improving plant growth and defense. It is also possible that defense metabolites are upregulated after accomplishing plant growth requirements in β CC-treated plants, which avoids diversion of carbon flux from growth toward defense. To examine this, we compared the metabolome of β CC-treated plants with control plants to reveal β CC-induced metabolic changes in tomato plants. In addition, we also compared β CC-induced metabolic changes with simulated-herbivory-induced changes to reveal β CC’s influence on the defense metabolites related to insect herbivory. Our results showed that β CC treatment mainly influenced the metabolism of amino acids and the accumulation of phytophenols.

Traditionally, amino acids are designated as the building blocks of protein; however, they also serve as intermediates for other biosynthetic pathways. Therefore, apart from plant growth and development, they also influence the generation of metabolic energy and signaling processes [37] and confer resistance to both abiotic and biotic stress [38–40]. In a recent study, it was demonstrated that pathogen-inoculated tomato plants’ primary metabolic pools were altered [41]. Similarly, β CC treatment induced many primary metabolites very early after the treatment. We found that β CC treatment increased the levels of tryptophan and its precursor shikimate. Shikimate is the common intermediate of the amino acid tryptophan and phenylalanine biosynthetic pathways. As tryptophan is the precursor for auxin and 5-hydroxytryptamine biosynthesis, an increase in the tryptophan level may contribute to plant growth. On the other hand, phenylalanine accumulation remained unaltered after β CC treatment; however, the derivatives of phenylalanine, namely, coumaric acid, rutin, and salicylic acid, were significantly increased (Figure 3a). These metabolites are known for their antioxidant and antipathogenic properties [42–44]. Moreover, rutin and coumaric acid application resulted in increased photosynthesis, chlorophyll content, and shoot growth [45,46]. In addition, the amino acids glutamate and glycine were also increased after β CC treatment. Glutamate is the precursor of chlorophyll tetrapyrrol protoporphyrin IX biosynthesis, where δ -aminolaevulinic acid (ALA) is the major intermediate [47]. Interestingly, the application of ^{14}C -labeled glycine can instantly be incorporated into ALA in dark-grown barley leaves [48]. Moreover, exogenous glycine application can stimulate root hair formation and [49] induce plant growth [50,51]. These findings are consistent with our previous results that showed that β CC treatment could enhance chlorophyll accumulation and root growth in tomato plants [11].

β CC treatment can also enhance the levels of aspartate, which serves as a precursor of many biosynthetic pathways required for growth and defense [52]. For example, it is a precursor for the aspartate oxidase pathway that synthesizes nicotinamide adenine dinucleotide (NAD), an essential component of chlorophyll synthesis [53]. Therefore, presumably, β CC-induced increase in glutamate, glycine, and aspartate accumulation supports increased chlorophyll content in β CC-treated plants. Another vital role of aspartate is to transfer the reduction equivalents from the glycolytic pathway to the mitochondria for ATP generation via the malate–aspartate shuttle [54]. Recent studies showed that mitochondrial components of the malate–aspartate NADH shuttle act as a longevity factor that induces the extension of lifespan in yeast. Therefore, presumably by enhancing the malate–aspartate shuttle, stress-induced excess reducing powers are ameliorated in mitochondria that ultimately helps plant survival during stress. Moreover, the accumulation of aspartate is closely related to stress acclimation. For example, aspartate concentration was increased significantly in drought-exposed *Brassica napus* plants [55]. It is known that out of the eight essential amino acids, four amino acids, namely methionine, threonine, lysine, and isoleucine, are produced from aspartate [56]. An increase in aspartate after β CC treatment is translated into an increase in the levels of homoserine (a common intermediate of methionine, threonine, and lysine), and specifically threonine, but not methionine, lysine, and isoleucine. β CC also induced the accumulation of leucine. An increase in threonine and leucine may be attributed to the critical components of serine/threonine protein kinases [57] and leucine-rich repeat (LRR) proteins [58], respectively, and facilitates the perception of stress signals and protein–protein interactions. An increase in the transcripts of serine/threonine protein kinases and LRR proteins after β CC application [25] suggests the same.

Abiotic stresses, such as drought and salinity, cause osmotic stress in the plant. To maintain osmolarity, plants produce compatible solutes to maintain cell turgor. These non-toxic compounds fall into three categories, namely, amino acids, onium compounds, and sugars/polyols [59]. Proline is one of the significant osmolytes; however, we found proline levels remained unaltered until three days after β CC treatment. Our previous study showed that proline significantly increased after 21 days of β CC treatment. Therefore proline may be upregulated after three days of β CC treatment. However, homoserine is a non-protein amino acid, and increased levels of homoserine can be attributed to the production of the homoserine betain, a known osmolyte in salt stress [60]. Mannose is another important metabolite that also works as an osmolyte and, in addition, enhances antioxidant metabolism and reduces chlorophyll degradation [61].

Accumulation of phytophenols is significantly increased after β CC treatment. They contribute to plant color and protect plants from oxidative stress, pathogen infestation, and herbivore attack [62]. Phytophenols are biosynthesized utilizing amino acids as the precursors; however, a few phenolic compounds are also derived from the shikimic acid pathway [63]. Coumaric acid is one of the phytophenols that is biosynthesized through the shikimate pathway [64] and can be converted into phenolic acids [65,66]. Therefore, an increase in the levels of coumaric acid and its phenolic acids, namely, ferulic acid and its isomer isoferulic acid, suggest a role of β CC in the production of defense metabolites against abiotic and biotic stress. This view is further strengthened by the commonly upregulated defense metabolites in β CC- and simulated-herbivory-treated samples. Interestingly, α -tomatine, a glycoalkaloid specifically present in tomato that deters insect herbivores, is significantly greater in β CC-treated plants than simulated-herbivory-treated plants. Similar trends were evident in the accumulation of quinic acid. Together, this suggests that β CC can upregulate defense metabolites that prime tomato plants against multiple stresses. However, a few metabolites, namely cinnamic acid, nicotinic acid, linoleic acid, solasodin, and solasonin, that are related to plant defense, were downregulated significantly. A high turnover of cinnamic acid to coumaric acid and rutin probably restricts its accumulation. Similarly, the allocation of aspartate towards homoserine production can limit aspartate allocation towards nicotinic acid. Downregulation of linoleic acid after β CC treatment is

surprising, as linoleic acid levels are known to be increased within an hour of herbivory and pathogen attack. After being attacked by herbivores, linoleic acid is liberated from cell membranes and is converted to jasmonate, which regulates transcription of the defense genes [67]. In our previous transcriptomic study, we did not find upregulation of any genes from the jasmonate biosynthetic cascade [25]. In the current study, we could not detect jasmonic acids or their derivatives; however, the levels of α -tomatine, a jasmonate-dependent glycoalkaloid [68], increased. Together, these suggest that β CC operates in a jasmonate-independent way in tomato plants. The other glycoalkaloids, solasodine, and solasonine were downregulated after BCC treatment. As α -tomatine is the major glycoalkaloid in tomato plants, downregulation of others may be cost-effective.

5. Conclusions

In the current study, we found that exogenous β CC elicits changes in the metabolome of tomato plants. Interestingly, these changes were more significant at early time points after β CC treatment than later ones. β CC mainly regulates amino acid and phytophenol metabolism. Interestingly, β CC-treated plants precisely upregulated metabolites having a role in improving both growth and defense; moreover, regulation of amino acid and phytophenol metabolism at different times optimized the growth of tomato plants. Therefore, β CC is a promising molecule for inducing resilience against biotic and abiotic stress. In general, most research has focused on the effect of priming molecules on plant phenotypic changes. However, our study sought to reveal the molecular changes that contribute to understanding the molecular mechanisms underlying priming.

Supplementary Materials: The following supporting information can be downloaded at: <https://www.mdpi.com/article/10.3390/metabo13030329/s1>; Figure S1: Representative base peak chromatogram (BPC) from LC-MS analysis of control, β CC-, and simulated-herbivory-treated samples; Figure S2: Fold-change analysis of the samples from early time points (0–240 min) after β CC treatment compared to control plants; Figure S3: Fold-change analysis of the samples from 72 h after β CC treated plants compared to control plants. Table S1: Compounds identified from control and β CC-treated tomato plants by LC-MS/MS; Table S2: Statistical analysis of the levels of discriminant metabolites identified early after β CC treatment.

Author Contributions: Conceptualization, S.M.; methodology, S.D.; software, S.D. and S.M.; validation, S.D. and S.M.; formal analysis, S.D. and S.M.; investigation, S.M.; resources, S.M.; data curation, S.M. and S.D.; writing—original draft preparation, S.M. and S.D.; writing—review and editing, S.M.; visualization, S.M.; supervision, S.M.; project administration, S.M.; funding acquisition, S.M. All authors have read and agreed to the published version of the manuscript.

Funding: This research was funded by the Ramalingaswami Reentry Fellowship, Department of Biotechnology (DBT), India. Grant number BT/HRD/35/02/2006.

Institutional Review Board Statement: Not applicable.

Informed Consent Statement: Not applicable.

Data Availability Statement: The data presented in this study are available in the main text and supplementary materials.

Acknowledgments: The authors acknowledge Savitribai Phule Pune University for the infrastructure provided for the study, V. T. Barvkar for technical help with LC-MS data acquisition, and S. Raskar, V. Purkar, and Rakesh M. for technical assistance.

Conflicts of Interest: The authors declare no conflict of interest. The funders had no role in the design of the study; in the collection, analyses, or interpretation of data; in the writing of the manuscript, or in the decision to publish the results.

References

- Thakur, B.; Singh, R.; Nelson, P. Quality attributes of processed tomato products: A review. *Food Rev. Int.* **1996**, *12*, 375–401. [[CrossRef](#)]
- Zhang, Y.; Song, H.; Wang, X.; Zhou, X.; Zhang, K.; Chen, X.; Liu, J.; Han, J.; Wang, A. The roles of different types of trichomes in tomato resistance to cold, drought, whiteflies, and botrytis. *Agronomy* **2020**, *10*, 411. [[CrossRef](#)]
- Nisar, N.; Li, L.; Lu, S.; Khin, N.C.; Pogson, B.J. Carotenoid metabolism in plants. *Mol. Plant* **2015**, *8*, 68–82. [[CrossRef](#)] [[PubMed](#)]
- Giuliano, G.; Al-Babili, S.; Von Lintig, J. Carotenoid oxygenases: Cleave it or leave it. *Trends Plant Sci.* **2003**, *8*, 145–149. [[CrossRef](#)]
- Hou, X.; Rivers, J.; León, P.; McQuinn, R.P.; Pogson, B.J. Synthesis and function of apocarotenoid signals in plants. *Trends Plant Sci.* **2016**, *21*, 792–803. [[CrossRef](#)]
- Verslues, P.E.; Agarwal, M.; Katiyar-Agarwal, S.; Zhu, J.; Zhu, J.K. Methods and concepts in quantifying resistance to drought, salt and freezing, abiotic stresses that affect plant water status. *Plant J.* **2006**, *45*, 523–539. [[CrossRef](#)]
- Moreno, J.C.; Mi, J.; Alagoz, Y.; Al-Babili, S. Plant apocarotenoids: From retrograde signaling to interspecific communication. *Plant J.* **2021**, *105*, 351. [[CrossRef](#)]
- Ramel, F.; Birtic, S.; Ginies, C.; Soubigou-Taconnat, L.; Triantaphylidès, C.; Havaux, M. Carotenoid oxidation products are stress signals that mediate gene responses to singlet oxygen in plants. *Proc. Natl. Acad. Sci. USA* **2012**, *109*, 5535–5540. [[CrossRef](#)]
- D'alessandro, S.; Ksas, B.; Havaux, M. Decoding β -cyclocitral-mediated retrograde signaling reveals the role of a detoxification response in plant tolerance to photooxidative stress. *Plant Cell* **2018**, *30*, 2495–2511. [[CrossRef](#)]
- d'Alessandro, S.; Mizokami, Y.; Legeret, B.; Havaux, M. The apocarotenoid β -cyclocitric acid elicits drought tolerance in plants. *Iscience* **2019**, *19*, 461–473. [[CrossRef](#)]
- Deshpande, S.; Manoharan, R.; Mitra, S. Exogenous β -cyclocitral treatment primes tomato plants against drought by inducing tolerance traits, independent of abscisic acid. *Plant Biol.* **2021**, *23*, 170–180. [[CrossRef](#)]
- Prasad, A.; Sedlářová, M.; Kale, R.S.; Pospišil, P. Lipoxygenase in singlet oxygen generation as a response to wounding: In vivo imaging in *Arabidopsis thaliana*. *Sci. Rep.* **2017**, *7*, 9831. [[CrossRef](#)] [[PubMed](#)]
- Mitra, S.; Estrada-Tejedor, R.; Volke, D.C.; Phillips, M.A.; Gershenson, J.; Wright, L.P. Negative regulation of plastidial isoprenoid pathway by herbivore-induced β -cyclocitral in *Arabidopsis thaliana*. *Proc. Natl. Acad. Sci. USA* **2021**, *118*, e2008747118. [[CrossRef](#)] [[PubMed](#)]
- Turner, M.F.; Heuberger, A.L.; Kirkwood, J.S.; Collins, C.C.; Wolfrum, E.J.; Broeckling, C.D.; Prenni, J.E.; Jahn, C.E. Non-targeted metabolomics in diverse sorghum breeding lines indicates primary and secondary metabolite profiles are associated with plant biomass accumulation and photosynthesis. *Front. Plant Sci.* **2016**, *7*, 953. [[CrossRef](#)]
- Dickinson, A.J.; Lehner, K.; Mi, J.; Jia, K.-P.; Mijar, M.; Dinneny, J.; Al-Babili, S.; Benfey, P.N. β -Cyclocitral is a conserved root growth regulator. *Proc. Natl. Acad. Sci. USA* **2019**, *116*, 10563–10567. [[CrossRef](#)]
- Reinhardt, D.; Kuhlemeier, C. Plant architecture. *EMBO Rep.* **2002**, *3*, 846–851. [[CrossRef](#)] [[PubMed](#)]
- Creydt, M.; Arndt, M.; Hudzik, D.; Fischer, M. Plant metabolomics: Evaluation of different extraction parameters for nontargeted UPLC-ESI-QTOF-mass spectrometry at the example of white *Asparagus officinalis*. *J. Agric. Food Chem.* **2018**, *66*, 12876–12887. [[CrossRef](#)]
- Piasecka, A.; Kachlicki, P.; Stobiecki, M. Analytical methods for detection of plant metabolomes changes in response to biotic and abiotic stresses. *Int. J. Mol. Sci.* **2019**, *20*, 379. [[CrossRef](#)]
- Shulaev, V.; Cortes, D.; Miller, G.; Mittler, R. Metabolomics for plant stress response. *Physiol. Plant.* **2008**, *132*, 199–208. [[CrossRef](#)]
- Zhao, Y.; Zhao, J.; Zhao, C.; Zhou, H.; Li, Y.; Zhang, J.; Li, L.; Hu, C.; Li, W.; Peng, X. A metabolomics study delineating geographical location-associated primary metabolic changes in the leaves of growing tobacco plants by GC-MS and CE-MS. *Sci. Rep.* **2015**, *5*, 16346. [[CrossRef](#)]
- Zielinska, A.; Siudem, P.; Paradowska, K.; Gralec, M.; Kaźmierski, S.; Wawer, I. Aronia melanocarpa fruits as a rich dietary source of chlorogenic acids and anthocyanins: 1H-NMR, HPLC-DAD, and chemometric studies. *Molecules* **2020**, *25*, 3234. [[CrossRef](#)]
- Jorge, T.F.; Mata, A.T.; António, C. Mass spectrometry as a quantitative tool in plant metabolomics. *Philos. Trans. R. Soc. A Math. Phys. Eng. Sci.* **2016**, *374*, 20150370. [[CrossRef](#)]
- De Vos, R.C.; Hall, R.D.; Moing, A. Metabolomics of a model fruit: Tomato. In *Annual Plant Reviews Online*; Volume 43: Biology of Plant Metabolomics; Wiley-Blacwell Ltd.: Oxford, UK, 2011; Volume 43, pp. 109–155.
- Zeiss, D.R.; Mhlongo, M.I.; Tugizimana, F.; Steenkamp, P.A.; Dubery, I.A. Metabolomic profiling of the host response of tomato (*Solanum lycopersicum*) following infection by *Ralstonia solanacearum*. *Int. J. Mol. Sci.* **2019**, *20*, 3945. [[CrossRef](#)]
- Deshpande, S.; Purkar, V.; Mitra, S. β -Cyclocitral, a Master Regulator of Multiple Stress-Responsive Genes in *Solanum lycopersicum* L. *Plants* **2021**, *10*, 2465. [[CrossRef](#)]
- Mitra, S.; Gershenson, J. Effects of herbivory on carotenoid biosynthesis and breakdown. *Methods Enzymol.* **2022**, *674*, 497–517.
- Hammer, Ø.; Harper, D.A.; Ryan, P.D. PAST: Paleontological statistics software package for education and data analysis. *Palaeontol. Electron.* **2001**, *4*, 9.
- Oliveros, J.C. VENNY. An Interactive Tool for Comparing Lists with Venn Diagrams. 2007. Available online: <http://bioinfogp.cnb.csic.es/tools/venny/index.html> (accessed on 1 December 2022).
- Fürstenberg-Hägg, J.; Zagrobelny, M.; Bak, S. Plant defense against insect herbivores. *Int. J. Mol. Sci.* **2013**, *14*, 10242–10297. [[CrossRef](#)] [[PubMed](#)]

30. Wasternack, C.; Stenzel, I.; Hause, B.; Hause, G.; Kutter, C.; Maucher, H.; Neumerkel, J.; Feussner, I.; Miersch, O. The wound response in tomato—role of jasmonic acid. *J. Plant Physiol.* **2006**, *163*, 297–306. [[CrossRef](#)] [[PubMed](#)]
31. Fujita, Y.; Fujita, M.; Shinozaki, K.; Yamaguchi-Shinozaki, K. ABA-mediated transcriptional regulation in response to osmotic stress in plants. *J. Plant Res.* **2011**, *124*, 509–525. [[CrossRef](#)] [[PubMed](#)]
32. Gamalero, E.; Glick, B.R. Ethylene and abiotic stress tolerance in plants. In *Environmental Adaptations and Stress Tolerance of Plants in the Era of Climate Change*; Springer: New York, NY, USA, 2012; pp. 395–412.
33. Loake, G.; Grant, M. Salicylic acid in plant defence—The players and protagonists. *Curr. Opin. Plant Biol.* **2007**, *10*, 466–472. [[CrossRef](#)] [[PubMed](#)]
34. Verma, V.; Ravindran, P.; Kumar, P.P. Plant hormone-mediated regulation of stress responses. *BMC Plant Biol.* **2016**, *16*, 86. [[CrossRef](#)] [[PubMed](#)]
35. Herms, D.A.; Mattson, W.J. The dilemma of plants: To grow or defend. *Q. Rev. Biol.* **1992**, *67*, 283–335. [[CrossRef](#)]
36. Abreu, A.C.; Fernández, I. NMR metabolomics applied on the discrimination of variables influencing tomato (*Solanum lycopersicum*). *Molecules* **2020**, *25*, 3738. [[CrossRef](#)] [[PubMed](#)]
37. Häusler, R.E.; Ludewig, F.; Krueger, S. Amino acids—a life between metabolism and signaling. *Plant Sci.* **2014**, *229*, 225–237. [[CrossRef](#)] [[PubMed](#)]
38. Moe, L.A. Amino acids in the rhizosphere: From plants to microbes. *Am. J. Bot.* **2013**, *100*, 1692–1705. [[CrossRef](#)] [[PubMed](#)]
39. Watanabe, M.; Balazadeh, S.; Tohge, T.; Erban, A.; Giavalisco, P.; Kopka, J.; Mueller-Roeber, B.; Fernie, A.R.; Hoefgen, R. Comprehensive dissection of spatiotemporal metabolic shifts in primary, secondary, and lipid metabolism during developmental senescence in Arabidopsis. *Plant Physiol.* **2013**, *162*, 1290–1310. [[CrossRef](#)]
40. Zeier, J. New insights into the regulation of plant immunity by amino acid metabolic pathways. *Plant Cell Environ.* **2013**, *36*, 2085–2103. [[CrossRef](#)]
41. Luna, E.; Flandin, A.; Cassan, C.; Prigent, S.; Chevanne, C.; Kadiri, C.F.; Gibon, Y.; Pétriacoq, P. Metabolomics to exploit the primed immune system of tomato fruit. *Metabolites* **2020**, *10*, 96. [[CrossRef](#)]
42. Zielinska, D.; Szawara-Nowak, D.; Zielinski, H. Determination of the antioxidant activity of rutin and its contribution to the antioxidant capacity of diversified buckwheat origin material by updated analytical strategies. *Pol. J. Food Nutr. Sci.* **2010**, *60*, 315–321.
43. Liu, X.; Ji, D.; Cui, X.; Zhang, Z.; Li, B.; Xu, Y.; Chen, T.; Tian, S. p-Coumaric acid induces antioxidant capacity and defense responses of sweet cherry fruit to fungal pathogens. *Postharvest Biol. Technol.* **2020**, *169*, 111297. [[CrossRef](#)]
44. Verberne, M.C.; Verpoorte, R.; Bol, J.F.; Mercado-Blanco, J.; Linthorst, H.J. Overproduction of salicylic acid in plants by bacterial transgenes enhances pathogen resistance. *Nat. Biotechnol.* **2000**, *18*, 779–783. [[CrossRef](#)]
45. Gorni, P.H.; de Lima, G.R.; de Oliveira Pereira, L.M.; Spera, K.D.; de Marcos Lapaz, A.; Pacheco, A.C. Increasing plant performance, fruit production and nutritional value of tomato through foliar applied rutin. *Sci. Hortic.* **2022**, *294*, 110755. [[CrossRef](#)]
46. Nkomo, M.; Gokul, A.; Keyster, M.; Klein, A. Exogenous p-coumaric acid improves *Salvia hispanica* L. seedling shoot growth. *Plants* **2019**, *8*, 546. [[CrossRef](#)] [[PubMed](#)]
47. Willows, R.D. Chlorophyll synthesis. In *The Structure and Function of Plastids*; Springer: Berlin/Heidelberg, Germany, 2007; pp. 295–313.
48. Hendry, G.A.; Stobart, A.K. Glycine metabolism and chlorophyll synthesis in barley leaves. *Phytochemistry* **1977**, *16*, 1567–1570. [[CrossRef](#)]
49. Domínguez-May, Á.V.; Carrillo-Pech, M.; Barredo-Pool, F.A.; Martínez-Estevez, M.; Us-Camas, R.Y.; Moreno-Valenzuela, O.A.; Echevarría-Machado, I. A novel effect for glycine on root system growth of habanero pepper. *J. Am. Soc. Hortic. Sci.* **2013**, *138*, 433–442. [[CrossRef](#)]
50. Kotinskyi, A.; Salyuk, A.; Zhadan, S. The influence of exogenous glycine on growth and cyanobacteria spirulina platensis (Gom.) Geitl photosynthetic processes. *Biotechnol. Acta* **2018**, *11*, 39–46. [[CrossRef](#)]
51. Mohammadipour, N.; Souri, M.K. Beneficial effects of glycine on growth and leaf nutrient concentrations of coriander (*Coriandrum sativum*) plants. *J. Plant Nutr.* **2019**, *42*, 1637–1644. [[CrossRef](#)]
52. Han, M.; Zhang, C.; Suglo, P.; Sun, S.; Wang, M.; Su, T. L-Aspartate: An essential metabolite for plant growth and stress acclimation. *Molecules* **2021**, *26*, 1887. [[CrossRef](#)]
53. Chai, M.-F.; Chen, Q.-J.; An, R.; Chen, Y.-M.; Chen, J.; Wang, X.-C. NADK2, an Arabidopsis chloroplastic NAD kinase, plays a vital role in both chlorophyll synthesis and chloroplast protection. *Plant Mol. Biol.* **2005**, *59*, 553–564. [[CrossRef](#)]
54. Borst, P. The malate–aspartate shuttle (Borst cycle): How it started and developed into a major metabolic pathway. *IUBMB Life* **2020**, *72*, 2241–2259. [[CrossRef](#)]
55. Good, A.G.; Zapłachinski, S.T. The effects of drought stress on free amino acid accumulation and protein synthesis in *Brassica napus*. *Physiol. Plant.* **1994**, *90*, 9–14. [[CrossRef](#)]
56. Li, Y.; Wei, H.; Wang, T.; Xu, Q.; Zhang, C.; Fan, X.; Ma, Q.; Chen, N.; Xie, X. Current status on metabolic engineering for the production of l-aspartate family amino acids and derivatives. *Bioresour. Technol.* **2017**, *245*, 1588–1602. [[CrossRef](#)] [[PubMed](#)]
57. Hardie, D. Plant protein serine/threonine kinases: Classification and functions. *Annu. Rev. Plant Biol.* **1999**, *50*, 97–131. [[CrossRef](#)] [[PubMed](#)]
58. Bella, J.; Hindle, K.; McEwan, P.; Lovell, S. The leucine-rich repeat structure. *Cell. Mol. Life Sci.* **2008**, *65*, 2307–2333. [[CrossRef](#)] [[PubMed](#)]

59. Nuccio, M.L.; Rhodes, D.; McNeil, S.D.; Hanson, A.D. Metabolic engineering of plants for osmotic stress resistance. *Curr. Opin. Plant Biol.* **1999**, *2*, 128–134. [[CrossRef](#)] [[PubMed](#)]
60. Kageyama, H.; Waditee-Sirisattha, R. Osmoprotectant molecules in cyanobacteria: Their basic features, biosynthetic regulations, and potential applications. In *Cyanobacterial Physiology*; Elsevier: Amsterdam, The Netherlands, 2022; pp. 113–123.
61. Zhao, S.; Zeng, W.; Li, Z.; Peng, Y. Mannose regulates water balance, leaf senescence, and genes related to stress tolerance in white clover under osmotic stress. *Biol. Plant.* **2020**, *64*, 406–416. [[CrossRef](#)]
62. Pratyusha, S. Phenolic Compounds in the Plant Development and Defense: An Overview. In *Plant Stress Physiology-Perspectives in Agriculture*; Intechopen Limited: London, UK, 2022; pp. 125–140.
63. Santos-Sánchez, N.F.; Salas-Coronado, R.; Hernández-Carlos, B.; Villanueva-Cañongo, C. Shikimic acid pathway in biosynthesis of phenolic compounds. In *Plant Physiological Aspects of Phenolic Compounds*; IntechOpen: London, UK, 2019; Volume 1, pp. 1–15.
64. Herrmann, K.M.; Weaver, L.M. The shikimate pathway. *Annu. Rev. Plant Biol.* **1999**, *50*, 473. [[CrossRef](#)]
65. El-Seedi, H.R.; El-Said, A.M.; Khalifa, S.A.; Goransson, U.; Bohlin, L.; Borg-Karlsson, A.-K.; Verpoorte, R. Biosynthesis, natural sources, dietary intake, pharmacokinetic properties, and biological activities of hydroxycinnamic acids. *J. Agric. Food Chem.* **2012**, *60*, 10877–10895. [[CrossRef](#)] [[PubMed](#)]
66. Pei, K.; Ou, J.; Huang, J.; Ou, S. p-Coumaric acid and its conjugates: Dietary sources, pharmacokinetic properties and biological activities. *J. Sci. Food Agric.* **2016**, *96*, 2952–2962. [[CrossRef](#)]
67. Conconi, A.; Miquel, M.; Browse, J.A.; Ryan, C.A. Intracellular levels of free linolenic and linoleic acids increase in tomato leaves in response to wounding. *Plant Physiol.* **1996**, *111*, 797–803. [[CrossRef](#)]
68. Panda, S.; Jozwiak, A.; Sonawane, P.D.; Szymanski, J.; Kazachkova, Y.; Vainer, A.; Vasuki Kilambi, H.; Almekias-Siegl, E.; Dikaya, V.; Bocobza, S. Steroidal alkaloids defence metabolism and plant growth are modulated by the joint action of gibberellin and jasmonate signalling. *New Phytol.* **2022**, *233*, 1220–1237. [[CrossRef](#)] [[PubMed](#)]

Disclaimer/Publisher's Note: The statements, opinions and data contained in all publications are solely those of the individual author(s) and contributor(s) and not of MDPI and/or the editor(s). MDPI and/or the editor(s) disclaim responsibility for any injury to people or property resulting from any ideas, methods, instructions or products referred to in the content.